Strong resonances on periodic arrays of cylinders and optical bistability with weak incident waves

Lijun Yuan*
College of Mathematics and Statistics, Chongqing Technology and Business University, Chongqing, China

Ya Yan Lu
Department of Mathematics, City University of Hong Kong, Hong Kong

A one-dimensional periodic array of circular dielectric cylinders surrounded by air is a simple structure on which guided modes above the lightline, also called bound states in the continuum (BICs), may exist. Recent studies reveal that such an array supports not only antisymmetric standing waves which are symmetry-protected BICs, but also propagating Bloch BICs and symmetric standing waves. Near a BIC, there is a family of resonant modes (depending on the Bloch wavenumber β) with arbitrarily large quality factors. Using a perturbation method, we show that the quality factor of the resonant mode typically depends on β like $1/(\beta-\beta_*)^2$, where β_* is the Bloch wavenumber the BIC, but near a symmetric standing wave ($\beta_* = 0$), the quality factor blows up like $1/\beta^4$. This indicates that strong resonances can be more easily induced near a symmetric standing wave. As an application, we numerically study optical bistability for the periodic array assuming the cylinders have a Kerr nonlinearity. With the nonlinear effects enhanced by the resonances, it is possible to have optical bistability for weak incident waves. The numerical results confirm that the weakest incident wave for optical bistability is realized through the resonances near the symmetric standing waves.

PACS numbers: 42.65.Hw,42.25.Fx,42.79.Dj

I. INTRODUCTION

Optical bistability (OB) is a classical nonlinear optical phenomenon that has been extensively studied in the last four decades [1]. The simplest nonlinear medium in which OB occurs is probably the Kerr medium, where the nonlinear effect is modeled by adding a term proportional to the field intensity to the linear dielectric constant. OB is proposed for a number of all-optical signal processing applications, such as optical switches and memory. However, the nonlinear coefficient of a conventional material is extremely small. In simple configurations, such as a slab of nonlinear medium, OB only occurs when the amplitude of the incident wave A is proportional to $1/\sqrt{\gamma}$ where γ is the nonlinear coefficient, unless the interaction length is very long. This implies that a device based on OB is either very large or requires a very high power for its operation. Clearly, such a device is not useful for nanophotonic applications.

One way to overcome these limitations is to enhance the nonlinear effects by a local field with a much larger amplitude than the incident wave. This can be achieved by resonances such as those in photonics crystal (PhC) microcavities [2–4]. When an incident wave with amplitude A excites a resonant mode with quality factor Q, the amplitude of the local field u is on the order of $\sqrt{Q}A$. In addition, the resonance induces sharp peaks or dips with an $O(1/Q)$ bandwidth in transmission, reflection or scattering spectra, and OB can occur when $\gamma|u|^2$ is on the order of Q^{-1}. Therefore, with the resonant enhancement, the required incident wave amplitude A for OB is proportional to $1/(Q\sqrt{\gamma})$ [5]. In principle, if resonant modes with arbitrarily large quality factors are utilized, OB can occur for arbitrarily weak incident waves. Some microcavities fabricated on PhC slabs indeed have resonant modes with very high quality factors, but once a microcavity is fabricated, its quality factor is fixed. To achieve OB at arbitrarily low incident field intensity, it is desirable to have a fixed physical structure on which a family of resonant modes exist, their quality factors tend to infinity, but their resonant frequencies converge to a constant. Notice that a simple resonator, such as a dielectric sphere, can not serve the purpose, since although it has a sequence of resonant modes with quality factors tending to infinity, the corresponding resonant frequencies also tend to infinity.

The desired family of resonant modes exist on periodic structures, such as PhC slabs and periodic arrays of cylinders. A periodic structure sandwiched between two homogeneous media could have guided modes that are confined around the main periodic part of the structure and decay exponentially into the surrounding homogeneous media. In addition to the well-known guided modes below the lightline, there could also be special guided modes above the lightline, i.e., their frequencies lie in the frequency intervals where radiation modes exist [6–20]. These guided modes above the lightline (i.e., in the radiation continuum) are special bound states in the continuum (BICs) [21–23], and mathematically they correspond to discrete eigenvalues in a continuous spectrum. On a two-dimensional (2D) structure with one periodic direction, resonant modes exist continuously with

* Corresponding author: ljyuan@ctbu.edu.cn

respect to the Bloch wavenumber β. It is known that the quality factor tends to infinity as β tends to the Bloch wavenumber β_* of a BIC. In fact, the quality factor is typically proportional to $1/(\beta-\beta_*)^2$. Therefore, resonant modes with arbitrarily large quality factors can be obtained if β is sufficiently close to β_*. In that case, for incident waves with a wavevector component equal to β, it is possible to have OB with very small incident wave amplitudes. However, this requires high precision for the incident wave vector.

A one-dimensional (1D) periodic array of parallel and infinitely long circular dielectric cylinders is a particular simple structure on which BICs exist [8, 16, 17, 20]. A well-known class of BICs are standing waves having a symmetry incompatible with that of the outgoing radiation modes. The existence of these so-called symmetry-protected BICs can be rigorously proved [6, 8, 17, 24]. The array also supports other BICs that are not protected by symmetry [16, 20]. For a fixed array, the BICs are isolated points in the frequency-wavenumber plane, but they exist continuously with respect to the radius and dielectric constant of the cylinders. In particular, for cylinders with their radius and the dielectric constant satisfying a proper condition, there are standing waves which are not protected by symmetry [16, 20].

In Sect. II, we describe the periodic array, present the the mathematical formulation, and recall some results on BICs. In Sect. III, we show that resonant modes near standing waves unprotected by symmetry have quality factors proportional to $1/(\beta-\beta_*)^4$, where $\beta_*=0$ and β (real and close to β_*) is the Bloch wavenumber of the resonant mode. This is very different from the resonant modes near ordinary BICs. The inverse fourth power relation indicates that the quality factor can be very large, even when $|\beta-\beta_*|$ is not so small. Consequently, resonant modes with high quality factors can be obtained with a much relaxed accuracy requirement for the wavenumber β. In Sect. IV, based on rigorous numerical simulations, we analyze OB enhanced by resonances near three distinct BICs. Numerical results for a fixed and small $|\beta-\beta_*|$ confirm that the minimum incident wave amplitude A for OB is proportional to $(\beta-\beta_*)^2/\sqrt{\gamma}$ for ordinary BICs and $(\beta-\beta_*)^4/\sqrt{\gamma}$ for the standing waves without symmetry protection.

II. FORMULATION AND BICS

In Fig. 1, we show a 1D periodic array of parallel and infinitely long circular cylinders surrounded by air. A Cartesian coordinate system is chosen so that the cylinders are parallel to the z axis, the array is periodic in y with period L, and the origin lies in the center of one cylinder. Therefore, the structure is symmetric with respect to both x and y axes. We assume that the cylinders are made from a dielectric material with a Kerr nonlinearity. The dielectric constant and the radius of the cylinders are ϵ_1 and a, respectively, where $\epsilon_1>1$ and $a<L/2$.

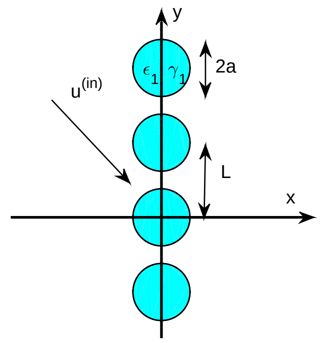

FIG. 1. A 1D array of circular cylinders with radius a, dielectric constant ϵ_1 and nonlinear coefficient γ_1. The array is periodic in y with period L.

For the E polarization, the z component of the electric field, denoted by u, satisfies the following nonlinear Helmholtz equation [25–30]:

$$\frac{\partial^2 u}{\partial x^2}+\frac{\partial^2 u}{\partial y^2}+k_0^2\left(\epsilon+\gamma|u|^2\right)u=0, \tag{1}$$

where $k_0=\omega/c$ is the free space wavenumber, ω is the angular frequency, c is the speed of light in vacuum, $\epsilon=\epsilon(\boldsymbol{r})$ is the dielectric function, $\boldsymbol{r}=(x,y)$, $\gamma=\gamma(\boldsymbol{r})$ is the nonlinear coefficient, and the time dependence is $e^{-i\omega t}$. In particular, we have $\epsilon=\epsilon_1$ and $\gamma=\gamma_1>0$ in the cylinders, and $\epsilon=1$ and $\gamma=0$ outside the cylinders. Equation (1) can be derived from the nonlinear Maxwell's equations with the assumption that higher harmonics can be ignored, and $\gamma=\frac{3}{4}\chi^{(3)}$ where $\chi^{(3)}$ is an element of the third order nonlinear susceptibility tensor.

We study the nonlinear diffraction problem for an incident plane wave given by

$$u^{(in)}(\boldsymbol{r})=Ae^{i\beta y+i\alpha(x+L/2)}, \quad x<-a, \tag{2}$$

where A is the amplitude, (α,β) is the wavevector, β is real, α is positive, and they satisfy $\alpha^2+\beta^2=k_0^2$. The reflected and transmitted waves can be expanded as

$$u^{(r)}(\boldsymbol{r})=\sum_{m=-\infty}^{\infty}c_m^-e^{i\beta_m y-i\alpha_m(x+L/2)},\ x<-a, \tag{3}$$

$$u^{(t)}(\boldsymbol{r})=\sum_{m=-\infty}^{\infty}c_m^+e^{i\beta_m y+i\alpha_m(x-L/2)},\ x>a, \tag{4}$$

where m is an integer, and

$$\beta_m=\beta+\frac{2\pi m}{L}, \quad \alpha_m=\sqrt{k_0^2-\beta_m^2}. \tag{5}$$

If $\alpha_0=\alpha$ is the only real number among all α_m, then the reflection and transmission coefficients for normalized power are

$$R=|c_0^-/A|^2, \quad T=|c_0^+/A|^2. \tag{6}$$

The nonlinear diffraction problem may have multiple solutions related to optical bistability and symmetry breaking phenomena [31]. To understand the nonlinear properties, it is necessary to first study the linear solutions of the periodic array. A BIC on the periodic array is a special Bloch mode solution of the linear Helmholtz equation [i.e. $\gamma \equiv 0$ in Eq. (1)] without any incident wave. It is given by

$$u(\boldsymbol{r}) = \phi(\boldsymbol{r}) e^{i\beta y}, \tag{7}$$

where ϕ is periodic in y with period L, $\phi \to 0$ as $|x| \to \infty$, and β is the real Bloch wavenumber (or propagation constant) satisfying $k_0 > |\beta|$ (i.e., above the lightline). Due to the periodicity of ϕ and the reflection symmetry in y, β can be restricted to the interval $[0, \pi/L]$. Notice that the array can be regarded as a periodic waveguide, and it has Bloch guided modes below the lightline (i.e., $k_0 < |\beta|$) that depend continuously on β and ω. On the other hand, the BICs only exist as isolated points in the frequency-wavenumber plane.

The simplest BICs on the periodic array shown in Fig. 1 are antisymmetric standing waves satisfying $\beta = 0$ and $u(x, -y) = -u(x, y)$ [16, 17]. The solution u given in Eq. (7) can be expanded in Fourier series for $|x| > a$, as in Eqs. (3) and (4). If $\beta = 0$ and $k_0 < 2\pi/L$, then α_0 is real and all other α_m for $m \neq 0$ are pure imaginary, and the only outgoing radiation channel is the plane wave for $m = 0$ in Eqs. (3) and (4). But if u is an odd function of y, the coefficients $c_0^{\pm}$ are zero automatically, thus $u \to 0$ as $|x| \to \infty$ is guaranteed. Since these antisymmetric standing waves have incompatible symmetry with the outgoing radiating waves, they are symmetry-protected BICs. However, the array also supports BICs that are not protected by symmetry, and they are propagating Bloch BICs with $\beta \neq 0$ or symmetric standing waves (even functions of y) [16, 20]. In particular, these Bloch BICs are quite robust, since they exist continuously with respect to the radius and dielectric constant of the cylinders [20].

In Fig. 2(a), we show a symmetry-protected BIC for $a = 0.382L$ and $\epsilon_1 = 5$. The normalized frequency of this standing wave is $\omega L/(2\pi c) = 0.532688$. For the same radius a and dielectric constant ϵ_1, there is a propagating Bloch BIC with normalized frequency $\omega L/(2\pi c) = 0.647949$ and normalized wavenumber $\beta L/(2\pi) = 0.07228$, and it is shown in Fig. 2(b). If we fix radius $a = 0.382L$ and allow ϵ_1 to vary, then we can find a family of BICs for $2.524 < \epsilon_1 \leq 6.44974$. Both ω and β depends continuously on ϵ_1. At the endpoint $\epsilon_1 = 6.44974$, we have $\beta = 0$ and $\omega L/(2\pi c) = 0.573935$, thus the Bloch BIC becomes a standing wave, and it has a symmetric (i.e., y-even) field pattern as shown in Fig. 2(c). From Figs. 2(b) and 2(c), we can see that this family of BICs without symmetry protection are even functions of x. It turns out that there is also a family of x-odd BICs for larger values of ϵ_1 [20].

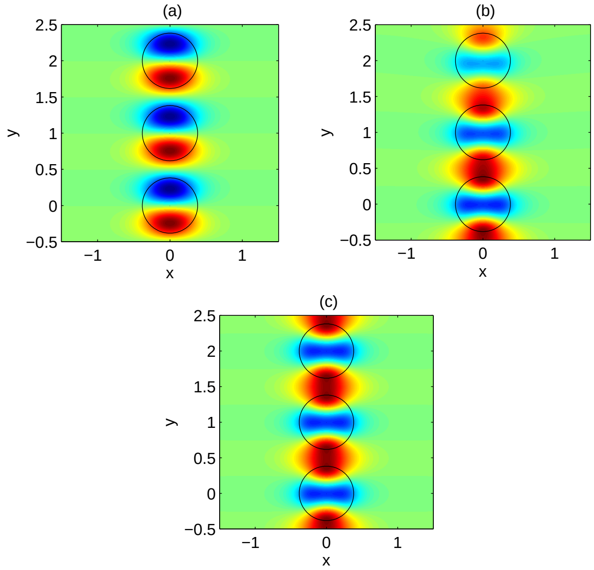

FIG. 2. Wave field patterns (i.e. the real parts of u) of three BICs on a periodic array of circular cylinders with radius $a = 0.382L$. (a) Antisymmetric (y-odd) standing wave for $\epsilon_1 = 5$ and $\omega L/(2\pi c) = 0.532688$; (b) Propagating BIC for $\epsilon_1 = 5$, $\omega L/(2\pi c) = 0.647949$ and $\beta L/(2\pi) = 0.07228$; (c) Symmetric (y-even) standing wave for $\epsilon_1 = 6.44974$ and $\omega L/(2\pi c) = 0.573935$. The x and y axis are given in unit L.

III. PERTURBATION ANALYSIS

For a fixed periodic array, a BIC corresponds to an isolated point in the ω-β plane. Let (ω_*, β_*) be a frequency-wavenumber pair of a BIC, then for any real β close to but not equal to β_*, the array has a resonant mode with a complex frequency ω near ω_*. A resonant mode is a nonzero solution of the linear Helmholtz equation (without incident waves) satisfying outgoing radiation conditions. Since we assume the time-dependence is $e^{-i\omega t}$, the imaginary part of the complex frequency, i.e., $\text{Im}(\omega)$, should be negative, so that the amplitude of the mode decays with time. The quality factor of the resonant mode is $Q = -0.5\text{Re}(\omega)/\text{Im}(\omega)$, where $\text{Re}(\omega)$ is the real part of ω. In the following, we show that if ω is expanded as a power series of $\beta - \beta_*$, then the first nonzero term in the series of $\text{Im}(\omega)$ is in general $(\beta - \beta_*)^2$, but it becomes $(\beta - \beta_*)^4$ for the symmetric (i.e. y-even) standing wave shown in Fig. 2(c).

First, we consider a general 2D periodic structure surrounded by air. We assume that the dielectric function $\epsilon(\boldsymbol{r})$ is real, is periodic in y with period L, and $\epsilon = 1$ for $|x| \geq L/2$. Let $u(\boldsymbol{r}) = e^{i\beta y}\phi(\boldsymbol{r})$ (for a complex frequency ω) be a resonant mode near a BIC $u_*(\boldsymbol{r}) = e^{i\beta_* y}\phi_*(\boldsymbol{r})$, we develop a perturbation theory for the resonant mode assuming $|\beta - \beta_*|$ is small. Since u belows up as $|x| \to \infty$, the perturbation theory should be developed in a bounded domain with proper boundary conditions for truncating x.

The linear Helmholtz equation for u gives rise to

$$\frac{\partial^2 \phi}{\partial x^2} + \frac{\partial^2 \phi}{\partial y^2} + 2i\beta \frac{\partial \phi}{\partial y} + (g\epsilon - \beta^2)\phi = 0, \tag{8}$$

where $g = k_0^2 = (\omega/c)^2$ is now complex. For $|x| \geq L/2$, we can expand u as in Eqs. (3) and (4). Comparing these expansions with their x derivatives at $x = \pm L/2$, we obtain the following boundary condition for ϕ [32]:

$$\pm \frac{\partial \phi}{\partial x} = \mathcal{T}\phi, \quad x = \pm \frac{L}{2}, \tag{9}$$

where $\mathcal{T}$ is a linear operator acting on periodic functions of y with period L, such that

$$\mathcal{T} e^{i2\pi m y/L} = \mu_m \, e^{i2\pi m y/L} \tag{10}$$

for all integers m and $\mu_m = i\sqrt{g - \beta_m^2}$. Since g is complex, the square root must be carefully defined. It is necessary to insist that the complex square root is continuous as $\beta \to \beta_*$ and $\omega \to \omega_*$ [or $g \to g_* = (\omega_*/c)^2$]. For simplicity, we assume $g_* - \beta_*^2 > 0$, and $g_* - \beta_{*m}^2 < 0$ for all $m \neq 0$, where $\beta_{*m} = \beta_* + 2\pi m/L$.

Let $\delta = \beta - \beta_*$, we expand ϕ, g, μ_m and operator $\mathcal{T}$ as follows

$$\phi = \phi_* + \delta\phi_1 + \delta^2\phi_2 + \ldots \tag{11}$$

$$g = g_* + \delta g_1 + \delta^2 g_2 + \ldots \tag{12}$$

$$\mu_m = \mu_{*m} + \delta\mu_{1m} + \delta^2\mu_{2m} + \ldots \tag{13}$$

$$\mathcal{T} = \mathcal{T}_* + \delta\mathcal{T}_1 + \delta^2\mathcal{T}_2 + \ldots \tag{14}$$

The explicit formulas for μ_{*m}, μ_{1m} and μ_{2m} are given in Appendix. Similar to the definition of $\mathcal{T}$ in Eq. (10), the actions of $\mathcal{T}_*$, $\mathcal{T}_1$ and $\mathcal{T}_2$ on $e^{i2\pi my/L}$ are simply $e^{i2\pi my/L}$ multiplied by μ_{*m}, μ_{1m} and μ_{2m}, respectively.

Inserting Eqs. (11), (12) and (14) into the governing equation (8) and boundary conditions (9), we get

$$\mathcal{L}\phi_* = 0, \tag{15}$$

$$\mathcal{L}\phi_1 = -2i\partial_y\phi_* + (2\beta_* - \epsilon g_1)\phi_*, \tag{16}$$

$$\mathcal{L}\phi_2 = -2i\partial_y\phi_1 + (2\beta_* - \epsilon g_1)\phi_1 + (1 - \epsilon g_2)\phi_*, \tag{17}$$

where

$$\mathcal{L} = \partial_x^2 + \partial_y^2 + 2i\beta_*\partial_y + g_*\epsilon - \beta_*^2, \tag{18}$$

and

$$\pm\partial_x\phi_* = \mathcal{T}_*\phi_*, \qquad x = \pm L/2, \tag{19}$$

$$\pm\partial_x\phi_1 = \mathcal{T}_*\phi_1 + \mathcal{T}_1\phi_*, \qquad x = \pm L/2, \tag{20}$$

$$\pm\partial_x\phi_2 = \mathcal{T}_*\phi_2 + \mathcal{T}_1\phi_1 + \mathcal{T}_2\phi_*, \quad x = \pm L/2. \tag{21}$$

Equations (15) and (19) are satisfied by the BIC. From Eqs. (16) and (20), we can show that

$$g_1 = \frac{2\beta_* \int_\Omega |\phi_*|^2 d\boldsymbol{r} - 2i \int_\Omega \overline{\phi}_* \partial_y \phi_* \, d\boldsymbol{r} + B_1}{\int_\Omega \epsilon |\phi_*|^2 \, d\boldsymbol{r} + B_0}, \tag{22}$$

where Ω is the square given by $|x| < L/2$ and $|y| < L/2$,

$$B_0 = \frac{L}{2} \sum_{m \neq 0} \frac{|c_{*m}^+|^2 + |c_{*m}^-|^2}{(\beta_{*m}^2 - g_*)^{1/2}}, \tag{23}$$

$$B_1 = L \sum_{m \neq 0} \beta_{*m} \frac{|c_{*m}^+|^2 + |c_{*m}^-|^2}{(\beta_{*m}^2 - g_*)^{1/2}}, \tag{24}$$

and $c_{*m}^\pm$ are the Fourier coefficients of ϕ_* at $x = \pm L/2$, i.e.,

$$\phi_*(\pm L/2, y) = \sum_{m=-\infty}^{\infty} c_{*m}^\pm \, e^{i2\pi my/L}. \tag{25}$$

The derivation of Eq. (22) is given in Appendix.

Since ϕ_* is period in y with period L, we have

$$0 = \int_\Omega \frac{\partial |\phi_*|^2}{\partial y} d\boldsymbol{r} = \int_\Omega \left[\phi_* \frac{\partial \overline{\phi}_*}{\partial y} + \overline{\phi}_* \frac{\partial \phi_*}{\partial y} \right] d\boldsymbol{r}.$$

Thus the term $2i \int_\Omega \overline{\phi}_* \partial_y \phi_* \, d\boldsymbol{r}$ in Eq. (22) is real. Since all other terms in Eq. (22) are clearly real, we conclude that g_1 is real. From Eq. (12), it is easy to get

$$\omega = \omega_* + \frac{c^2 g_1}{2\omega_*}\delta + O(\delta^2). \tag{26}$$

Therefore, $\mathrm{Im}(\omega)$ is in general $O(\delta^2)$ and the quality factor is proportional to $1/\delta^2$.

Next, we consider resonant modes near standing waves ($\beta_* = 0$) on symmetric (i.e. y-even) periodic structures. If $u(x,y) = e^{i\beta y}\phi(x,y)$ is a resonant mode on such a structure, then so is its reflection $u(x,-y) = e^{-i\beta y}\phi(x,-y)$. This implies that if the resonant mode is non-degenerate, ω (also g) should be an even function of β. Thus, Eq. (12) becomes

$$g = g_* + \delta^2 g_2 + \delta^4 g_4 + \ldots \tag{27}$$

where $\delta = \beta$. We can also apply the reflection transform to standing waves. This leads to the conclusion that a standing wave ϕ_* on a symmetric periodic structure must be either symmetric (y-even) or antisymmetric (y-odd), since otherwise, we can construct them from $\phi_*(x,y) + \phi_*(x,-y)$ or $\phi_*(x,y) - \phi_*(x,-y)$. The results shown in Figs. 2(a) and (c) confirm this conclusion. Whether ϕ_* is symmetric or antisymmetric, $\overline{\phi}_* \partial_y \phi_*$ is always odd in y, thus $\int_\Omega \overline{\phi}_* \partial_y \phi_* d\boldsymbol{r} = 0$. Moreover, the Fourier coefficients satisfy $|c_{*m}^\pm| = |c_{*,-m}^\pm|$, $\beta_{*m} = 2\pi m/L$, thus $B_1 = 0$. From Eq. (22), we again conclude that $g_1 = 0$.

The equations for ϕ_1 and ϕ_2 are simplified as

$$\mathcal{L}\phi_1 = -2i\partial_y\phi_*, \tag{28}$$

$$\mathcal{L}\phi_2 = (1 - \epsilon g_2)\phi_* - 2i\partial_y\phi_1, \tag{29}$$

where $\mathcal{L} = \partial_x^2 + \partial_y^2 + g_*\epsilon$. In Appendix, we show that

$$g_2 = \frac{\int_\Omega \left[|\phi_*|^2 - |\nabla\phi_1|^2 + g_*\epsilon|\phi_1|^2 \right] d\boldsymbol{r} - B_2 + B_3}{\int_\Omega \epsilon |\phi_*|^2 d\boldsymbol{r} + B_0}, \tag{30}$$

where B_0 is given in Eq. (23),

$$B_2 = \frac{Lg_*}{2}\sum_{m\neq 0}\frac{|c^+_{*m}|^2+|c^-_{*m}|^2}{(\beta^2_{*m}-g_*)^{3/2}} \tag{31}$$

$$B_3 = L\sum_m \overline{\mu}_{*m}(|c^+_{1m}|^2+|c^-_{1m}|^2), \tag{32}$$

and $c^{\pm}_{1m}$ are the Fourier coefficients of ϕ_1 at $x=\pm L/2$, that is

$$\phi_1(\pm L/2, y) = \sum_{m=-\infty}^{\infty} c^{\pm}_{1m} e^{i2\pi m y/L}. \tag{33}$$

Moreover, $\mu_{*0} = i\sqrt{g_*-\beta_*^2} = i\omega_*/c$ is pure imaginary, and all μ_{*m}, for $m\neq 0$, are real and given in Appendix. Equation (27) implies that

$$\omega = \omega_* + \frac{c^2 g_2}{2\omega_*}\delta^2 + O(\delta^4) \tag{34}$$

for standing waves. Thus,

$$\mathrm{Im}(\omega) = -\frac{Lc\left(|c^+_{10}|^2+|c^-_{10}|^2\right)}{2\left(\int_\Omega \epsilon|\phi_*|^2\, d\boldsymbol{r} + B_0\right)}\delta^2 + O(\delta^4). \tag{35}$$

For a y-even standing wave ϕ_*, we notice that $\mathcal{T}_1\phi_*$ in Eq. (20) is odd in y, $\partial_y\phi_*$ in Eq. (28) is also odd in y, thus ϕ_1 is an odd function of y, the coefficients $c^{\pm}_{10}$ vanish, and $\mathrm{Im}(g_2)=0$. As a result, we have $\mathrm{Im}(\omega)=O(\delta^4)$ and the quality factor is proportional to $1/\delta^4$.

For the three BICs shown in Fig. 2, we calculate the complex resonant frequency ω for some β close to β_*. In Fig. 3, we show the relations between the normalized

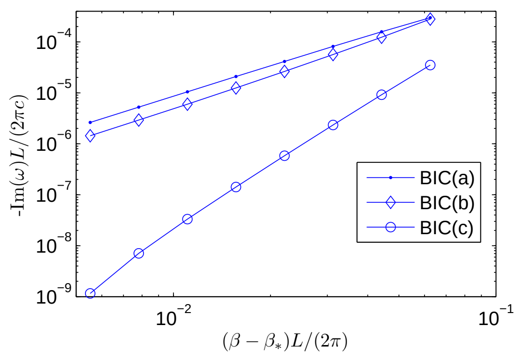

FIG. 3. Logarithmic relations between $-\mathrm{Im}(\omega)L/(2\pi c)$ and $(\beta-\beta_*)L/(2\pi)$ for the three BICs shown in Fig. 2.

$-\mathrm{Im}(\omega)$ and normalized $\beta-\beta_*$ in a logarithmic scale. It can be seen that the two curves for the antisymmetric standing wave and the propagating BIC have a relatively small slope (close to 2), while the curve for the symmetric standing wave has a larger slope (close to 4). These numerical results confirm the theoretical results developed in this section.

IV. OPTICAL BISTABILITY

In this section, we consider the nonlinear diffraction problem formulated in Sect. II for a periodic array of circular cylinders with the Kerr nonlinearity. Since resonances with arbitrarily high quality factors can be obtained when the wavenumber β is close to the wavenumber β_* of a BIC, we consider incident waves with a real frequency ω and a real wavevector (α,β), where ω is close to the frequency ω_* of the BIC, and β is close to β_*. It should be pointed that OB is a robust nonlinear optical phenomenon. Its appearance does not sensitively depend on the choice of ω. For the three BICs shown in Fig. 2, especially the symmetric standing wave shown in Fig. 2(c), we show that OB occurs for incident waves with small amplitudes if $|\beta-\beta_*|$ is small.

For the linear problem ($\gamma\equiv 0$), let Q be the quality factor of the resonant mode with a real wavenumber β and a complex frequency ω_c, and A be the amplitude of the incident wave with the real frequency $\omega=\mathrm{Re}(\omega_c)$ and the real wave vector (α,β), then the field amplitude around the array is $O(\sqrt{Q}A)$ [33]. In addition, a linear perturbation theory shows that if ϵ_1 of the cylinders is slightly increased, the real part of the complex frequency ω_c decreases slightly. For the nonlinear problem, the term $\gamma|u|^2$ effectively increases the dielectric constant ϵ_1 of the cylinders, thus the most dramatic resonance enhancement occurs at a real frequency ω slightly smaller than $\mathrm{Re}(\omega_c)$.

Although OB has been widely studied, it is difficult to predict the precise values of the incident amplitude A for which OB actually occurs. However, it is possible to obtain some estimates based on related linear problems. Due to the coupling of the incident plane wave with the resonant mode, the linear transmission or reflection spectrum for a fixed β typically exhibits an asymmetric lineshape for frequencies around $\mathrm{Re}(\omega_c)$. Furthermore, the spectrum contains two frequencies around $\mathrm{Re}(\omega_c)$ for total transmission and total reflection, respectively, and the difference between these two frequencies is $O(1/Q)$ [33, 34]. It appears that OB can only occur when the nonlinear term $\gamma|u|^2$ induces an $O(1/Q)$ shift in the resonant frequency, i.e., the resonant frequency $\tilde{\omega}_c$ for $\tilde{\epsilon}_1=\epsilon_1+\gamma|u|^2$ differs from the original ω_c by an $O(1/Q)$ amount. In addition, to the first order, $\tilde{\omega}_c-\omega_c$ varies linearly with $\tilde{\epsilon}_1-\epsilon_1$. Therefore, OB requires that $\gamma_1|u|^2=O(\gamma_1 QA^2)=O(1/Q)$, or

$$A = O\left(\frac{1}{Q\sqrt{\gamma_1}}\right). \tag{36}$$

Based on the results of Sect. III, we conclude that near a typical BIC, OB may occur when

$$A = O\left(\frac{(\beta-\beta_*)^2L^2}{\sqrt{\gamma_1}}\right), \tag{37}$$

but near the symmetric standing wave, the condition becomes

$$A = O\left(\frac{\beta^4 L^4}{\sqrt{\gamma_1}}\right). \tag{38}$$

For the three BICs shown in Fig. 2, we solve the nonlinear diffraction problem assuming the incident wavevector component β satisfies $(\beta - \beta_*)L/(2\pi) = 0.01$ and the nonlinear coefficient of the cylinders is $\gamma_1 = 1.125 \times 10^{-17}\,\mathrm{m}^2/\mathrm{V}^2$. The first BIC is the antisymmetric standing wave shown in Fig. 2(a). Its normalized frequency is $\omega_* L/(2\pi c) = 0.532688$. For the β given above ($\beta_* = 0$), the array has a resonant mode with complex frequency $\omega_c L/(2\pi c) = 0.532479 - 0.0000086i$. The corresponding quality factor is $Q \approx 3.1 \times 10^4$. The frequency of the incident wave is chosen to be $\omega L/(2\pi c) = 0.53246$. In Fig. 4, we show a curve relating the reflection coefficient R and

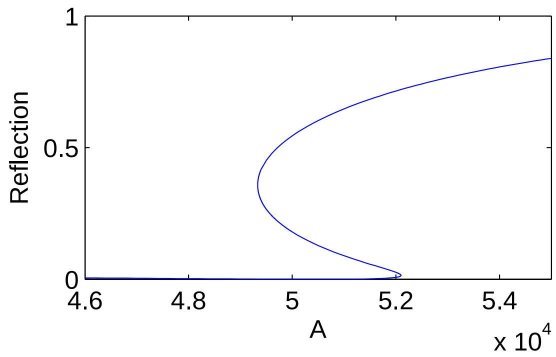

FIG. 4. Reflection coefficient of a nonlinear diffraction problem related to the BIC shown in Fig. 2(a), for different incident amplitude A (with unit V/m), wavenumber $\beta L/(2\pi) = 0.01$ and frequency $\omega L/(2\pi c) = 0.53246$.

the incident amplitude A. For A between 4.93×10^4 and $5.21 \times 10^4\,\mathrm{V/m}$, R has multiple values corresponding to the multiple solutions related to the OB phenomenon.

The second BIC is the propagating mode shown in Fig. 2(b). Its frequency and wavenumber are $\omega_* L/(2\pi c) = 0.647949$ and $\beta_* L/(2\pi) = 0.07228$, respectively. For β given above, there is a resonant mode with complex frequency $\omega_c L/(2\pi c) = 0.650409 - 0.0000048i$. The corresponding quality factor is $Q \approx 6.8 \times 10^4$. For incident waves with frequency $\omega L/(2\pi c) = 0.65040$ and the given β, we solve the nonlinear diffraction problem and obtain the multi-valued amplitude-dependent reflection coefficient R shown in Fig. 5. Notice that OB occurs when A is between 2.73×10^4 and $2.81 \times 10^4\,\mathrm{V/m}$.

The third BIC shown in Fig. 2(c) is the symmetric standing wave on an array with radius $a = 0.382L$ and dielectric constant $\epsilon_1 = 6.44974$. Its frequency is $\omega_* L/(2\pi c) = 0.573935$. For $\beta L/(2\pi) = 0.01$, the array has a resonant mode with complex frequency $\omega_c L/(2\pi c) = 0.574086 - 0.000000022i$ and quality factor $Q \approx 1.3 \times 10^7$. For incident waves with frequency $\omega L/(2\pi c) \approx 0.574086$ and the given β, we find the relation between reflection coefficient R and amplitude A

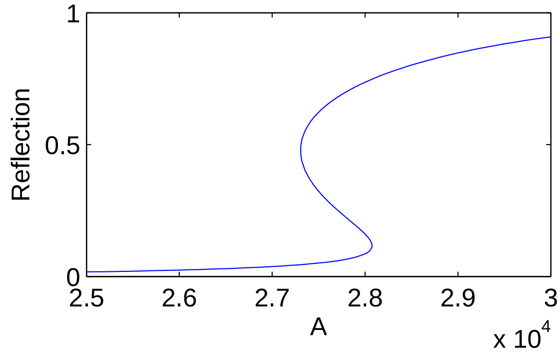

FIG. 5. Reflection coefficient of a nonlinear diffraction problem related to the BIC shown in Fig. 2(b), for different incident amplitude A (with unit V/m), wavenumber $\beta L/(2\pi) = 0.08228$ and frequency $\omega L/(2\pi c) = 0.65040$.

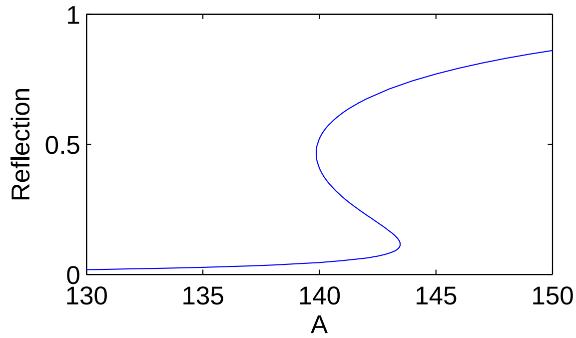

FIG. 6. Reflection coefficient of a nonlinear diffraction problem related to the BIC shown in Fig. 2(c), for different incident amplitude A (with unit V/m), wavenumber $\beta L/(2\pi) = 0.01$ and frequency $\omega L/(2\pi c) \approx 0.574086$.

as shown in Fig. 6. We can see that OC occurs for A between 139.9 and 143.5 V/m. Compared with the two previous cases, a much weak incident wave is needed to realize OB, even though $\beta - \beta_*$ is identical in all three cases.

V. CONCLUSION

On periodic structures such as an array of circular cylinders, there could be special guided modes in the radiation continuum, and they are referred to as BICs. Near a BIC with Bloch wavenumber β_*, there are resonant modes that depend continuously on a given Bloch wavenumber β. As $\beta \to \beta_*$, the resonant frequencies of these modes converge to that of the BIC, and their quality factors tend to infinity. Using a perturbation theory, we show that for a typical BIC, the quality factors is proportional to $1/(\beta - \beta_*)^2$, but for a symmetric standing wave ($\beta_* = 0$) on a symmetric periodic structure, the quality factors is proportional to $1/\beta^4$. The latter case is particularly interest, since it gives rise to strong resonances with a relaxed requirement on β.

As an application of the resonances near the BICs, we study optical bistability for single arrays of circular cylinders with a Kerr nonlinearity. Since the nonlinear coefficient of a conventional dielectric material is very small, usually OB is only possible for very strong incident waves. With resonance enhancement, the required incident wave amplitude for OB can be significantly reduced. Since the quality factors of the resonant modes near a BIC can be arbitrarily high, in principle, OB can happen for incident waves with arbitrarily low intensity. Our numerical results for three different BICs and the same $\beta - \beta_*$ confirm that the smallest incident amplitude needed for OB can be realized by resonances near a symmetric standing wave.

It should be pointed out that the existence of BICs and nearby resonances with arbitrarily high quality factors requires an infinite structure with perfect periodicity. In practice, the array is always finite, the cylinders are not perfectly identical, the length of the cylinders is also finite, and the incident wave cannot be a true plane wave. Clearly, it is important to study these practical issues. For a finite array of possibly distorted cylinders, the resonant modes form a discrete sequence, but it is worthwhile to find out whether there are particularly strong resonances when the related ideal periodic array supports symmetric standing waves. It is also highly relevant to consider incident waves with a finite beam-width, and study optical bistability when the frequency and the main wavevector of the beam are related to different kinds of BICs.

ACKNOWLEDGMENTS

The authors acknowledge support from the National Natural Science Foundation of China (11201508), the Natural Science Foundation of Chongqing (cstc2016jcyjA0491, 2013jcyjA20015), the Scientific and Technological Research Program of Chongqing Municipal Education Commission (KJ110712), the Program for University Innovation Team of Chongqing (CXTDX201601026), and the Research Grants Council of Hong Kong Special Administrative Region, China (Grant No. CityU 11301914).

APPENDIX

The perturbation theory is developed for resonant modes near a BIC on a 2D periodic structure with a dielectric function $\epsilon(x, y)$, where ϵ is real, periodic in y with period L, and $\epsilon = 1$ for $x \geq L/2$. A BIC is a special solution $u_* = e^{i\beta_* y}\phi_*$ for a real frequency ω_*. For a real β close to but not equal to β_*, the linear Helmholtz equation has a resonant mode $u = e^{i\beta y}\phi$ for a complex ω near ω_*, where ϕ is periodic in y and satisfies the outgoing radiation condition (9). The perturbation theory is developed for $g = (\omega/c)^2$ and ϕ, assuming $\delta = \beta - \beta_*$ is small. The operator $\mathcal{T}$ appeared in the boundary condition (9) is related to μ_m which has been expanded in Eq. (13). For $m = 0$, we have

$$\mu_{*0} = i\sqrt{g_* - \beta_*^2},$$
$$\mu_{10} = \frac{i(g_1 - 2\beta_*)}{2\sqrt{g_* - \beta_*^2}},$$
$$\mu_{20} = \frac{i(g_2 - 1)}{2\sqrt{g_* - \beta_*^2}} - \frac{i(g_1 - 2\beta_*)^2}{8(g_* - \beta_*^2)^{3/2}}.$$

For $m \neq 0$, we have

$$\mu_{*m} = -\sqrt{\beta_{*m}^2 - g_*},$$
$$\mu_{1m} = \frac{g_1 - 2\beta_{*m}}{2\sqrt{\beta_{*m}^2 - g_*}},$$
$$\mu_{2m} = \frac{g_2 - 1}{2\sqrt{\beta_{*m}^2 - g_*}} + \frac{(g_1 - 2\beta_{*m})^2}{8(\beta_{*m}^2 - g_*)^{3/2}}.$$

Based on the expansions for ϕ, g and $\mathcal{T}$, we obtain the equations and boundary conditions for ϕ_*, ϕ_1 and ϕ_2.

Multiplying Eq. (16) by $\overline{\phi}_*$ (the complex conjugate of ϕ_*), and integrating the result on the square Ω (given by $|x| < L/2$ and $|y| < L/2$), we obtain

$$\int_\Omega \overline{\phi}_* \mathcal{L}\phi_1 d\boldsymbol{r} = -2i\int_\Omega \overline{\phi}_* \frac{\partial \phi_*}{\partial y} d\boldsymbol{r} + 2\beta_* \int_\Omega |\phi_*|^2 d\boldsymbol{r} - g_1 \int_\Omega \epsilon |\phi_*|^2 d\boldsymbol{r}. \quad (39)$$

For the left hand side above, we notice that

$$\overline{\phi}_* \mathcal{L}\phi_1 = \phi_1 \overline{\mathcal{L}\phi_*} + \nabla \cdot (\overline{\phi}_* \nabla \phi_1 - \phi_1 \nabla \overline{\phi}_*) + 2i\beta_* \partial_y (\overline{\phi}_* \phi_1).$$

The first term in the right hand side vanishes. Due to the periodicity in y, the integral of the last term on Ω is zero. Using Green's theorem, we obtain

$$\int_\Omega \overline{\phi}_* \mathcal{L}\phi_1 d\boldsymbol{r} = \int_{\partial\Omega} \left[\overline{\phi}_* \frac{\partial \phi_1}{\partial \nu} - \phi_1 \frac{\partial \overline{\phi}_*}{\partial \nu} \right] ds,$$

where $\partial\Omega$ is the boundary of Ω, ν is the outward unit normal vector of $\partial\Omega$, ∂_ν becomes ∂_y, $-\partial_y$, $-\partial_x$ and ∂_x on the top, bottom, left and right edges of Ω, respectively. Due to the periodicity in y, the line integral on the top and bottom edges cancel out. Using the boundary conditions (19) and (20), we obtain

$$\int_\Omega \overline{\phi}_* \mathcal{L}\phi_1 d\boldsymbol{r} = J(F_0) + J(F_1) = J(F_1), \quad (40)$$

where

$$F_0 = \overline{\phi}_* (\mathcal{T}_* \phi_1) - \phi_1 (\overline{\mathcal{T}_* \phi_*}), \quad F_1 = \overline{\phi}_* \mathcal{T}_1 \phi_*,$$

and for each integer j,

$$J(F_j) = \int_{-L/2}^{L/2} [F_j(L/2, y) + F_j(-L/2, y)]\, dy. \quad (41)$$

Since ϕ_* decays to zero as $|x| \to \infty$, we have $c_{*0}^{\pm} = 0$, where $c_{*m}^{\pm}$ are the Fourier coefficients of ϕ_* at $x = \pm L/2$, as in Eq. (25). In addition, μ_{*m} (for $\mathcal{T}_*$) is real if $m \neq 0$. Using these results, we can verify that $J(F_0) = 0$. Using the Fourier series of ϕ_* at $x = \pm L/2$ and the definition of $\mathcal{T}_1$, we obtain

$$J(F_1) = g_1 B_0 - B_1, \tag{42}$$

where B_0 and B_1 are given in Eqs. (23) and (24), respectively. Combining Eqs. (39), (40) and (42), we obtain Eq. (22) for g_1.

Next, we assume that the periodic structure has a reflection symmetry along the y axis, i.e., ϵ is an even function of y, and consider resonant modes around a standing wave ϕ_* which is either symmetric (even in y) or anti-symmetric (odd in y). Due to the symmetry, g is an even function of δ. The conditions $\beta_* = 0$ and $g_1 = 0$ lead to some simplifications. Notice that $\beta_{*m} = 2\pi m/L$, and for $m \neq 0$,

$$\mu_{1m} = \frac{-\beta_{*m}}{\sqrt{\beta_{*m}^2 - g_*}},$$
$$\mu_{2m} = \frac{g_2}{2\sqrt{\beta_{*m}^2 - g_*}} + \frac{g_*}{2(\beta_{*m}^2 - g_*)^{3/2}}.$$

Multiplying Eq. (29) by $\overline{\phi}_*$ and integrating the result on Ω, we obtain

$$\int_\Omega \overline{\phi}_* \mathcal{L}\phi_2 d\boldsymbol{r} = \int_\Omega |\phi_*|^2 d\boldsymbol{r} - g_2 \int_\Omega \epsilon|\phi_*|^2 d\boldsymbol{r} - 2i \int_\Omega \overline{\phi}_* \frac{\partial \phi_1}{\partial y} d\boldsymbol{r}. \tag{43}$$

For the left hand side, we notice that

$$\overline{\phi}_* \mathcal{L}\phi_2 = \phi_2 \overline{\mathcal{L}\phi_*} + \nabla \cdot (\overline{\phi}_* \nabla \phi_2 - \phi_2 \nabla \overline{\phi}_*).$$

This leads to

$$\begin{aligned}\int_\Omega \overline{\phi}_* \mathcal{L}\phi_2 \, d\boldsymbol{r} &= \int_{\partial\Omega} \left[\overline{\phi}_* \frac{\partial \phi_2}{\partial \nu} - \phi_2 \frac{\partial \overline{\phi}_*}{\partial \nu} \right] ds \\ &= J(F_2) + J(F_3) + J(F_4) \\ &= J(F_2) + J(F_3),\end{aligned}$$

where

$$\begin{aligned}F_2 &= \overline{\phi}_* \mathcal{T}_2 \phi_*, \\ F_3 &= \overline{\phi}_* \mathcal{T}_1 \phi_1, \\ F_4 &= \overline{\phi}_* \mathcal{T}_* \phi_2 - \phi_2 (\overline{\mathcal{T}_* \phi_*}),\end{aligned}$$

and $J(F_j)$, for $j = 2, 3, 4$, are defined in Eq. (41). In the above, we notice that the line integrals on the top and bottom edges of Ω cancel out, the boundary conditions (19) and (21) are applied, and $J(F_4) = 0$. Therefore, we can rewrite Eq. (43) as

$$\begin{aligned}&2i \int_\Omega \overline{\phi}_* \frac{\partial \phi_1}{\partial y} d\boldsymbol{r} + J(F_3) \\ &= \int_\Omega |\phi_*|^2 d\boldsymbol{r} - g_2 \int_\Omega \epsilon |\phi_*|^2 d\boldsymbol{r} - J(F_2).\end{aligned} \tag{44}$$

Multiplying Eq. (28) by $\overline{\phi}_1$, integrating the result on Ω, and taking a complex conjugate, we obtain

$$2i \int_\Omega \phi_1 \frac{\partial \overline{\phi}_*}{\partial y} d\boldsymbol{r} = \int_\Omega \left[g_* \epsilon |\phi_1|^2 - |\nabla \phi_1|^2 \right] d\boldsymbol{r} + J(F_5) + J(F_6) \tag{45}$$

where $F_5 = \phi_1 \overline{\mathcal{T}_* \phi_1}$, $F_6 = \phi_1 \overline{\mathcal{T}_1 \phi_*}$. Using the properties of ϕ_* and $\mathcal{T}_*$ mentioned above, we can verify that

$$J(F_6) = J(F_3).$$

In addition, we notice that

$$\int_\Omega \left[\overline{\phi}_* \frac{\partial \phi_1}{\partial y} + \phi_1 \frac{\partial \overline{\phi}_*}{\partial y} \right] d\boldsymbol{r} = \int_\Omega \frac{\partial (\overline{\phi}_* \phi_1)}{\partial y} d\boldsymbol{r} = 0.$$

Therefore, Eq. (45) can be written as

$$\begin{aligned}&2i \int_\Omega \overline{\phi}_* \frac{\partial \phi_1}{\partial y} d\boldsymbol{r} + J(F_3) \\ &= \int_\Omega \left[|\nabla \phi_1|^2 - g_* \epsilon |\phi_1|^2 \right] d\boldsymbol{r} - J(F_5).\end{aligned} \tag{46}$$

Using the Fourier series of ϕ_* and ϕ_1 at $x = \pm L/2$ and the definitions of $\mathcal{T}_*$ and $\mathcal{T}_2$, we obtain

$$J(F_2) = L \sum_m \mu_{2m} (|c_{*m}^+|^2 + |c_{*m}^-|^2) = g_2 B_0 + B_2,$$
$$J(F_5) = L \sum_m \overline{\mu}_{*m} (|c_{1m}^+|^2 + |c_{1m}^-|^2) = B_3,$$

where B_0, B_2 and B_3 are defined in Sect. III. The formula for g_2, i.e., Eq. (30), can be easily obtained from the above two equations, and Eqs. (45), (46).

[1] H. Gibbs, *Optical Bistability: Controlling Light with Light* (Academic, 1985).

[2] C. M. Bowden and A. M. Zheltikov, "Nonlinear optics of photonic crystals," J. Opt. Soc. Am. B **19**, 2046–2048 (2002).

[3] M. Soljačić and J. D. Joannopoulos, "Enhancement of nonlinear effects using photonic crystals," Nat. Mater. **3**, 211–219 (2004).

[4] J. Bravo-Abad, A. Rodriguez, P. Bermel, S. G. Johnson, J. D. Joannopoulos, and M. Soljačić, "Enhance nonlinear optics in photonic-crystal microcavities," Opt. Express **15**, 16161–16176 (2007).

[5] M. Soljačić, M. Ibanescu, S. G. Johnson, Y. Fink, and J. D. Joannopoulos, “Optimal bistable switching in nonlinear photonic crystals,” Phys. Rev. E **66**, 055601(R) (2002).

[6] A.-S. Bonnet-Bendhia and F. Starling, “Guided waves by electromagnetic gratings and nonuniqueness examples for the diffraction problem,” Math. Methods Appl. Sci. **17**, 305-338 (1994).

[7] R. Porter and D. Evans, “Embedded Rayleigh-Bloch surface waves along periodic rectangular arrays,” Wave Motion **43**, 29-50 (2005).

[8] S. Shipman and D. Volkov, “Guided modes in periodic slabs: existence and nonexistence,” SIAM J. Appl. Math. **67**, 687–713 (2007).

[9] D. C. Marinica, A. G. Borisov, and S. V. Shabanov, “Bound states in the continuum in photonics,” Phys. Rev. Lett. **100**, 183902 (2008).

[10] R. F. Ngangali and S. V. Shabanov, “Electromagnetic bound states in the radiation continuum for periodic double arrays of subwavelength dielectric cylinders,” J. Math. Phys. **51**, 102901 (2010).

[11] J. Lee, B. Zhen, S. L. Chua, W. Qiu, J. D. Joannopoulos, M. Soljačić, and O. Shapira, “Observation and differentiation of unique high-Q optical resonances near zero wave vector in macroscopic photonic crystal slabs,” Phys. Rev. Lett. **109**, 067401 (2012).

[12] C. W. Hsu, B. Zhen, S.-L. Chua, S. G. Johnson, J. D. Joannopoulos, and M. Soljačić, “Bloch surface eigenstates within the radiation continuum,” Light Sci. Appl. **2**, e84 (2013).

[13] C. W. Hsu, B. Zhen, J. Lee, S.-L. Chua, S. G. Johnson, J. D. Joannopoulos, and M. Soljačić, “Observation of trapped light within the radiation continuum,” Nature **499**, 188–191 (2013).

[14] Y. Yang, C. Peng, Y. Liang, Z. Li, and S. Noda, “Analytical perspective for bound states in the contnuum in photonic crystal slabs,” Phys. Rev. Lett. **113**, 037401 (2014).

[15] B. Zhen, C. W. Hsu, L. Lu, A. D. Stone, and M. Soljačić, “Topological nature of optical bound states in the contnuum,” Phys. Rev. Lett. **113**, 257401 (2014).

[16] E. N. Bulgakov and A. F. Sadreev, “Bloch bound states in the radiation continuum in a periodic array of dielectric rods,” Phys. Rev. A **90**, 053801 (2014).

[17] Z. Hu and Y. Y. Lu, “Standing waves on two-dimensional periodic dielectric waveguides,” Journal of Optics **17**, 065601 (2015).

[18] L. Yuan and Y. Y. Lu, “Nonlinear standing waves on a periodic array of circular cylinders,” Opt. Express **23**(16), 20636–20646 (2015).

[19] C. W. Hsu, B. Zhen, A. D. Stone, J. D. Joannopoulos, and M. Soljačić, “Bound states in the continuum,” Nat. Rev. Mater. **1**, 16048 (2016).

[20] L. Yuan and Y. Y. Lu, “Propagating Bloch modes above the lightline on a periodic array of cylinders,” submitted to J. Phys. B.

[21] J. von Neumann and E. Wigner, “über merkwürdige diskrete Eigenwerte,” Phys. Z **30**, 465–467 (1929).

[22] F. H. Stillinger and D. R. Herrick, “Bound states in the continuum,” Phys. Rev. A **11**, 446–454 (1975).

[23] H. Friedrich and D. Wintgen, “Physical realization of bound states in the continuum,” Phys. Rev. A **31**, 3964 (1985).

[24] D. V. Evans, M. Levitin and D. Vassiliev, “Existence theorems for trapped modes,” J. Fluid Mech. **261**, 21–31 (1994).

[25] R. W. Boyd, *Nonlinear Optics*, 3rd ed. (Academic, 2008).

[26] E. Centeno and D. Felbacq, “Optical bistability in finite-size nonlinear bidimensional photonic crystals doped by a microcavity,” Phys. Rev. B **62**, R7683–R7686 (2000).

[27] B. Maes, P. Bienstman, and R. Baets, “Modeling of Kerr nonlinear photonic components with mode expansion,” Opt. Quant. Electron. **36**, 15–24 (2004).

[28] G. Bao, Y. Lia, and H. Wu, “Numerical solution of nonlinear diffraction problems,” J. Comput. Appl. Math. **190**, 170–189 (2006).

[29] G. Baruch, G. Fibich, and S. Tsynkov, “A high-order numerical method for the nonlinenar Helmholtz equation in multi-dimensional layered media,” J. Comput. Phys. **228**, 3789–3815 (2009).

[30] L. Yuan and Y. Y. Lu, “Efficient numerical method for analyzing optical bistability in photonic crystal microcavities,” Opt. Express **21**, 11952–11964 (2013).

[31] L. Yuan and Y. Y. Lu, “Diffraction of plane waves by a periodic array of nonlinear circular cylinders,” Phys. Rev. A **94,** 013852 (2016)

[32] G. Bao, D. C. Dobson and J. A. Cox, “ Mathematical studies in rigorous grating theory, ” J. Opt. Soc. Am. A **12**, 1029-1042 (1995).

[33] S. P. Shipman and S. Venakides, “Resonant transmission near nonrobust periodic slab modes,” Phys. Rev. E **71**, 026611 (2005).

[34] S. Shipman and H. Tu, “Total resonant transmission and reflection by periodic structures,” SIAM J. Appl. Math. **72**, 216-239 (2012).